ELSEVIER

Journal of Nuclear Materials 266–269 (1999) 611–617

journal of nuclear materials

Radiation efficiency of high power ergodic divertor plasmas in Tore Supra

P. Monier-Garbet *, C. DeMichelis, Ph. Ghendrih, R. Giannella, C. Grisolia, A. Grosman, R. Guirlet, J. Gunn, F. Laugier, B. Meslin, R. Reichle, J. C. Vallet

Association Euratom-CEA sur la fusion, Département de Recherches sur la Fusion Contrôlée, Centre d'études de Cadarache, F-13108 Saint-Paul-lez-Durance, France

Abstract

Highly radiative edge layer experiments in Tore Supra ergodic divertor (ED) plasmas are reported. In these experiments, up to 88% of the injected power is radiated in steady state attached plasma conditions. The observed radiated power is higher than the prediction of Matthews' multi-machine scaling. Such behaviour is consistent with the fact that the ratio of the ergodic divertor volume to the main plasma volume is higher for an ergodic divertor than for axisymmetric divertors, or with the enhanced impurity screening observed in Tore Supra. Indeed, a new scaling is derived for impurity radiation in a region of parallel ion transport. It shows that impurity screening is the dominant mechanism controlling divertor radiation, impurity transport along the open field lines having only little influence on P_{rad}. © 1999 Elsevier Science B.V. All rights reserved.

Keywords: Divertor radiation; Parallel ion transport; Impurity screening; Divertor detachment

1. Introduction

Highly radiating edge steady state regimes have been investigated for several years in tokamaks because they are considered to be a solution to the excessive heat load on the plasma facing components of the next tokamak generation. In divertor configurations, either axisymmetric divertors or ergodic divertors (ED), present experiments seek to maximize radiation in the divertor region where the physics is controlled by parallel transport and atomic processes. The level of divertor radiation is determined by the electron density in the divertor volume, the impurity concentration in this region, and the parallel electron temperature gradient. Therefore, the more straightforward method to increase radiation is to increase the electron density. Another method consists in operating at a lower electron density, and injecting additional impurities. These impurities should ionize on the open field lines of the divertor volume, so that they radiate in this region without contaminating the confined plasma. In Tore Supra, the ergodic divertor configuration is used to produce highly radiative edge plasmas at reduced core contamination. The high radiation efficiency (ratio of radiated power to plasma core contamination) of the ED configuration has already been reported [1,2]. The experiments analysed in this paper are aimed at determining the maximum power that it is possible to radiate in the edge in steady state conditions, for a given value of the total injected power, and for the particle and heat transport established in the edge by the ergodic divertor configuration. ICRH is used for additional heating. This method, contrary to neutral beam injection heating, is sensitive to plasma edge conditions; therefore, the maximum electron density achievable in steady state conditions is given by the onset of plasma detachment from the divertor target plates and ICRH antennae (note that in the ED configuration, the ICRH antennae are located within the divertor volume). The detachment is defined here by the roll-over of the target plate density (n_e^{div}) [3], and an electron temperature on the target plates in the 10 eV range [1]. Indeed, a good coupling of the ICRH waves

* Corresponding author. Tel.: +33-4 42 25 61 37; fax: +33-4 42 25 62 33; e-mail: monier@132.169.8.117

0022-3115/99/$ – see front matter © 1999 Elsevier Science B.V. All rights reserved.
PII: S0022-3115(98)00593-5

requires that the electron density just in front of the antennae remains sufficiently high. In our experiments, a feedback technique is used to maintain steady state conditions just before detachment. Both strategies are investigated to increase radiation: increasing the plasma electron density up to the detachment limit, or injecting light impurities (N, Ne). The effect of adding different impurity gases on divertor detachment has also recently been reported from Alcator C-Mod [4]. In Section 2, the model [5,6] that we have used to describe impurity radiation in the divertor region of parallel ion transport is presented. Section 3 describes the experimental scenario used on Tore Supra. In Section 4, the radiation capability with ICRH is determined as a function of the radiating impurity. In Section 5, the relation found experimentally on Tore Supra between the radiated power, the effective charge of the plasma core, and the central line averaged electron density ($\bar{n}_e$) is compared to the multi-machine scaling [7]. More insight into the physics understanding of the observed radiated power is obtained through the parallel ion transport model for impurity radiation.

2. Model for impurity radiation in a region of parallel transport

The simple model which is presented in the following has been used already by other authors [5,6]. Its purpose throughout this paper is only to provide a guide for the analysis of our experiments. The parallel heat flux balance equation is

$$\frac{\mathrm{d}Q_\parallel}{\mathrm{d}s} = -n_e n_Z L_Z(T_e) \tag{1}$$

with

$$Q_\parallel = -\kappa_\parallel \frac{\mathrm{d}T_e}{\mathrm{d}s}, \tag{2}$$

where L_Z is the impurity radiative power loss coefficient, and $\kappa_\parallel = \kappa_0 T_e^{2.5}$ is the parallel heat conductivity. From Eqs. (1) and (2), one can derive

$$Q_{\parallel 1}^2 - Q_{\parallel 0}^2 = 2p_e^2 c_{Z,0}\kappa_0 \int_{T_0}^{T_1} T_e^{0.5} L_Z(T_e)\,\mathrm{d}T_e, \tag{3}$$

where Q_1 is the incident power flux at the separatrix, and Q_0 the conducted–convected power flux at the target plate. p_e is the electron pressure, constant along a field line, and $c_{Z,0}$ is the impurity concentration in the divertor volume. We have assumed here that $c_{Z,0}$ is constant along a field line. T_1 and T_0 are the electron temperatures at the last closed magnetic surface and at the target plate, respectively. If the conducted–convected power at the target plate is small compared to the incident power flux ($Q_{\parallel 0} \ll Q_{\parallel 1}$), then the maximum radiated power is proportional to $Q_{\parallel 1}$:

$$P_{\mathrm{rad}} \propto \sqrt{c_{Z,0}}\, n_0 T_0 \sqrt{\int_{T_0}^{T_1} T_e^{0.5} L_Z(T_e)\,\mathrm{d}T_e}, \tag{4}$$

n_0 being the electron density on the neutralizer target plate. This model is similar to that given in Ref. [8] where the radiated energy per impurity particle is introduced to describe radiation in a region of perpendicular transport. On the open field lines of the divertor region, impurity transport is rapid compared to the time to approach coronal equilibrium. The impurity parallel lifetime is of the order of $\tau_\parallel = \lambda_{\mathrm{ion}}/v_{\mathrm{th}Z} \approx 1$ ms, and $n_e\tau_\parallel \approx 1 \times 10^{16}$ s m^{-3}. Consequently, the radiative power loss coefficient to be used in Eq. (4) is larger than at coronal equilibrium. This effect has been taken into account to calculate the expression

$$I(T_0) = \sqrt{\int_{T_0}^{T_1} T_e^{0.5} L_Z(T_e)\,\mathrm{d}T_e}$$

for T_0 in the range 10–100 eV and $T_1 \approx 100$ eV corresponding to the measured electron temperature in the vicinity of the last closed magnetic surface. The result is plotted on Fig. 1 for C, N, O and Ne. It shows that, within the model assumptions, namely an impurity concentration constant along a field line, the predicted radiated power increases weakly at low values of T_0:$I(T_0)$ increases by a factor $\leqslant 1.5$ for T_0 decreasing from 30 to 10 eV. The model also predicts the fraction of radiated power $P_{\mathrm{rad}}/P_{\mathrm{tot}} = (Q_{\parallel 1} - Q_{\parallel 0})/Q_{\parallel 1}$ at the onset of detachment, $T_0 \approx 10$ eV. The result is compared to experiment in Section 4.

3. Experiment

In the first series of experiments (Fig. 2) reported in this paper, a density ramp is obtained by injecting either pure deuterium gas or a mixture of deuterium and a small quantity of nitrogen. The fraction of nitrogen atoms in the injected gas varies between 3% and 10% from shot to shot. In order to determine the operational limits of this scenario, the gas injection is carried on up to disruption which occurs for a central line average electron density decreasing from $\bar{n}_e = 5.8 \times 10^{19}$ m^{-3} for pure deuterium injection, to 4.7×10^{19} m^{-3} when the mixture with 10% nitrogen is puffed. In a second series of experiments, 2 s steady state conditions are achieved for $\bar{n}_e \approx 4.5 \times 10^{19}$ m^{-3}, using neon injection. Fig. 3 shows an example of such a shot. The radiation increase is obtained by puffing a mixture of deuterium and 10% neon. The density ramp is stopped just before detachment occurs, when the ratio of the signals on the two outermost vertically viewing bolometer chords reaches 90% of the detachment threshold. Steady state

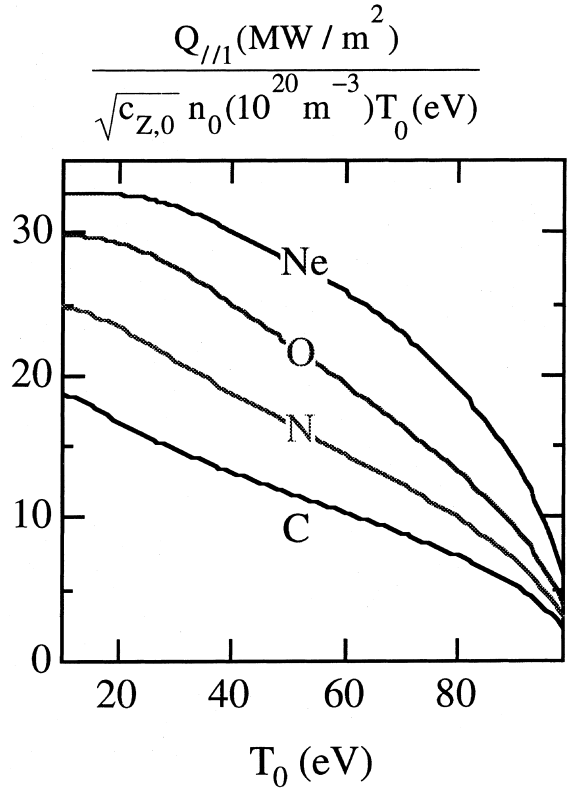

Fig. 1. Model calculation of the integral $I(T_0)$ for C, N, O and Ne impurities. Rapid impurity transport with $n_e\tau_{\parallel} = 1 \times 10^{16}$ s m^{-3} is assumed.

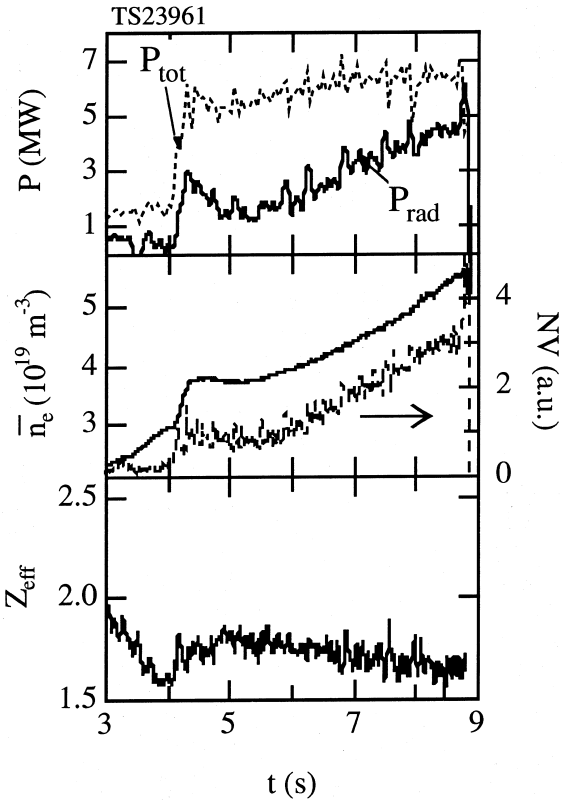

Fig. 2. Time evolution for a shot in the first series of experiments, showing the density ramp with 3% of nitrogen in the injected gas.

conditions are then achieved using a feedback control of the gas injection by the total radiated power [9]. The neon injection can be controlled, due to the neon pumping capability of the turbo-molecular pumps installed on the outboard modular limiter. In these experiments, the total injected power is close to 6.5 MW in the first series (respectively 7.5 MW in the second series), obtained by 5 MW (respectively 6 MW) of ICRH power in the minority heating scenario, and 1.5 MW of ohmic heating. The toroidal magnetic field is $B_t \approx 3.0$ T, the plasma minor radius $a = 0.78$ m, and the resonant value of the edge safety factor $q_\psi(a) \approx 3.1$. The current in the ED coils is set at its maximum value $I_{ED} = 45$ kA, corresponding to an average magnetic perturbation $\langle \delta B_r \rangle / B_t \approx 1.5 \times 10^{-3}$.

The measurement of the power exhaust balance is of primary importance. In our experiments, the conducted–convected power to the divertor target plates ($P_{cond} \propto Q_{\parallel 0}$) is measured by infrared thermography. The target plates are actively cooled copper tubes protected by a B_4C coating of thickness $e = 170$ μm. Therefore, the conducted–convected power is directly proportional to the temperature difference (ΔT) between the surface and the coolant: $P_{cond} = (\lambda/e) \times \Delta T \times s$, where λ is the thermal conductivity of the B_4C coating (1.7 W m^{-1} K^{-1}), and s is the wetted surface area. s has been estimated to be ≈ 0.6 m^2, taking into account the inhomogeneity of the power deposition on a neutralizer, and the deposition of part of the conducted–convected power on the front face of the ED. In the experiments described here, ΔT is measured for one target plate only, and the total conducted–convected power is calculated assuming toroidal symmetry of the deposition pattern. The result is in agreement with global calorimetric measurements. The radiated power is then deduced by $P_{rad} = P_{tot} - P_{cond} - (dW/dt)$, where P_{tot} is the total power coupled to the confined plasma. For the ICRH minority heating scenario used in these experiments, 10–20% of the injected power, depending on the exact position of the absorption layer and on the plasma collisionality, is estimated (a more precise determination is under way) to be lost through energetic particles trapped in the toroidal magnetic field ripple. This effect is taken into account for the determination of P_{tot}. We have

estimated that the absolute error on the determination of P_{rad} by this power balance method is $\approx 20\%$. Tore Supra is also equipped with three bolometer camera arrays at different poloidal and toroidal locations. However, difficulties are encountered in the interpretation of these measurements in terms of a global radiated power due to important differences in the measurements by the three cameras [10]. Therefore in this paper, bolometer data are used only to measure the radiation pattern, and give an estimate of the ratio of the divertor radiation to the total radiation.

The separate contributions of the dominant light impurities (C, O, and N) to the total radiated power are deduced from VUV spectroscopy of the low charge state ions, CIV (24.49 nm), OIV (23.85 nm) and NV (24.76 nm). The contamination of the plasma core is estimated from the measurement of the effective charge by visible bremsstrahlung, and the separate contributions of the light impurities to Z_{eff} are deduced from VUV spectroscopy of the Lyα lines of the H-like ions. The electron density and temperature on the neutralizer plates are measured by a set of dedicated fixed Langmuir probes.

4. Experimental determination of the radiation capability with ICRH

In the first series of experiments, the disruption occurs for a central line average electron density ($\bar{n}_e^{max}$) decreasing as the fraction of nitrogen in the injected gaz increases (Fig. 4(a)). In these shots, density regimes comparable to that found in axisymmetric divertors [3,11] are observed: first, a high recycling regime where $n_e^{div} \propto (\bar{n}_e)^3$ is found for $\bar{n}_e < 0.8 \times \bar{n}_e^{max}$. It is followed by a partially detached regime characterized by the beginning of the roll-over of the target plate density, before the final decrease of n_e^{div} and the disruption when the plasma fully detaches from the ICRH antennae and divertor target plates. Simultaneaously, the electron temperature on the target plates falls in the 10 eV range. Fig. 5 shows the evolution of the measured radiated power during the density ramp versus the inverse target plate temperature ($1/T_e^{div}$). The radiated power increases up to the point where $T_e^{div} \approx 14$ eV. Then, the control of the radiative layer is lost, and the disruption occurs for $T_e^{div} \approx 10$ eV. Bolometer data show that approximately 80% of the total radiation comes from the divertor

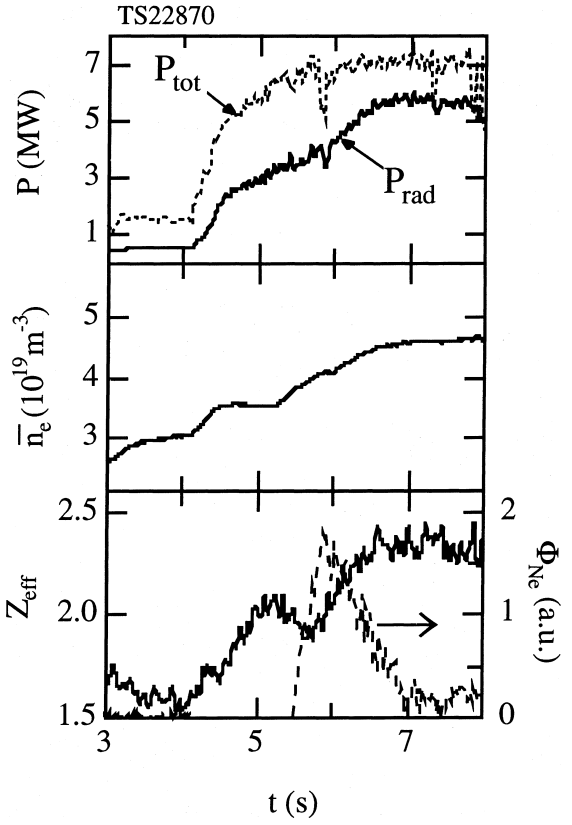

Fig. 3. Time evolution of TS22870, 2 s steady state highly radiating phase with neon injection.

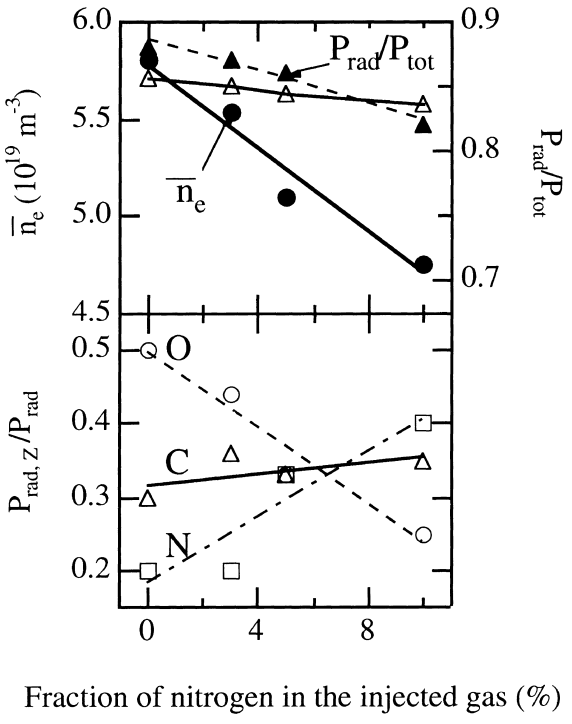

Fig. 4. (a) Maximum central line average electron density and fraction of radiated power achieved before detachment versus fraction of nitrogen in the injected gas. Full and open triangles: P_{rad}/P_{tot} from experiment and model calculation, respectively. (b) Separate contributions of O, N and C to P_{rad}.

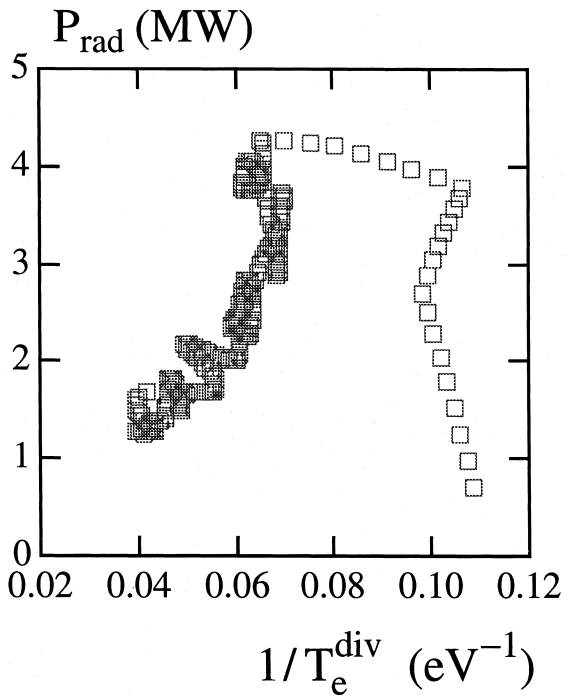

Fig. 5. Evolution of the measured radiated power with the inverse target plate electron temperature.

volume. During the high recycling, partially detached and detached regimes, radiation shifts from the low field side close to the target plates, to a radiating shell shifted inwards but remaining within the divertor volume [1]. The maximum fraction of radiated power achieved in these shots decreases from $P_{rad}/P_{tot} \approx 88\%$ for pure deuterium injection, oxygen being the main radiator (Fig. 4(b)), to $\approx 82\%$ when radiation is mainly due to nitrogen. The difference between the two cases is small. However, even if the absolute error on the determination of P_{rad}/P_{tot} can reach $\approx 20\%$, the precision on the relative values is sufficiently high for the observed difference to be representative of a physics effect. Indeed, oxygen radiation allows a higher radiated power than nitrogen because it occurs at a higher temperature, $T_e \approx 20$ eV, compared to ≈ 10 eV for nitrogen (coronal equilibrium values), and therefore a larger fraction of the power that it is possible to radiate with oxygen is actually radiated before detachment occurs. This effect is predicted by the parallel ion transport model described in Section 2, the result of the calculation being compared to the experiment in Fig. 4(a). The model also predicts that neon allows an even higher fraction of radiated power before detachment occurs, as the maximum of radiation for neon occurs for $T_e \approx 40$ eV. In our second series of experiments with neon injection (Fig. 3), $P_{rad}/P_{tot} \approx 83\%$ is achieved in up to 2 s steady state conditions. No divertor detachment is observed, the electron temperature on the fixed divertor Langmuir probes remaining higher than ≈ 15 eV. However, since the density ramp has not been continued up to detachment in these shots, the maximum value of P_{rad}/P_{tot} has not been determined for neon radiation. These experiments show that, for $P_{tot} \approx 6$ MW, it is possible to radiate up to approximately 88% of this power in a controlled experimental scenario (attached plasma conditions), if the dominant radiator is oxygen. This maximum radiation is obtained by increasing the electron density up to $\bar{n}_e \approx 5.8 \times 10^{19}$ m^{-3}. If operation at a lower electron density is required, nitrogen or neon injections can be used, nitrogen producing only a slightly lower value of the maximum achievable fraction of radiated power.

5. Scaling of radiated power with target plate electron temperature

In this section, the radiated power achieved in our experiments is compared to the multi-machine scaling, $P_{rad}^{mm} = 0.12 \times \bar{n}_e^2 \times (Z_{eff} - 1) \times S$, proposed by Matthews in Ref. [7]. $\bar{n}_e$ is the central line averaged electron density, and S the plasma surface area. The measured

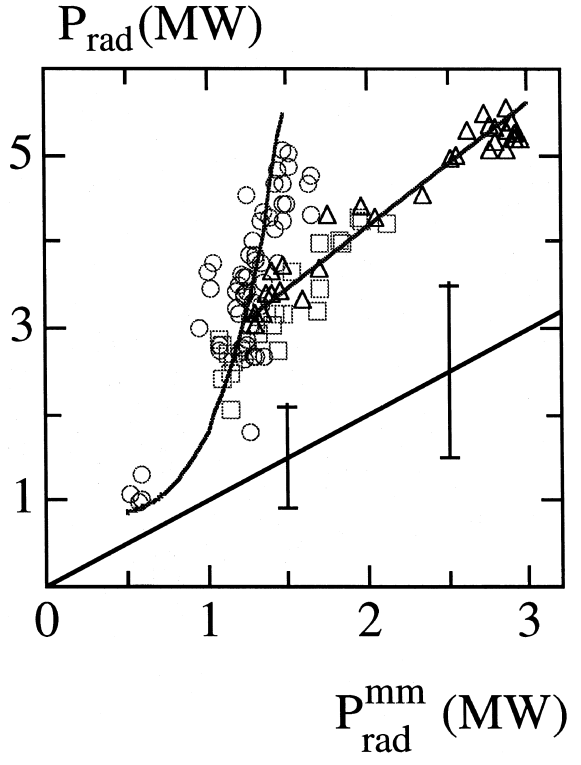

Fig. 6. Measured radiated power versus prediction of the multi-machine scaling (solid line). Circles: deuterium injection. Squares: density ramp with 10% nitrogen in the injected gas. Triangles: density ramp with 10% neon.

radiated power is plotted in Fig. 6 versus the prediction of the multi-machine scaling (P_{rad}^{mm}), for three typical ED shots with a density ramp and either deuterium, nitrogen or neon injection. The data with $P_{rad} < 1.6$ MW correspond to the ohmic phase of the plasmas and are correctly described by the multi-machine scaling. For $P_{rad} > 1.6$ MW, corresponding to the ICRH phase of the plasmas, the measured radiated power is higher than the multi-machine prediction by a factor $H_{rad} \equiv P_{rad}/P_{rad}^{mm} = 3$ in the case of pure deuterium injection, or $H_{rad} = 2$ in the case of nitrogen or neon injection. In trying to understand this deviation from the multi-machine scaling, we have considered the following facts. First, the multi-machine scaling implicitly assumes that the electron density in the radiating volume (n_e^{rad}) is proportional to $\bar{n}_e$. However in the divertor region, n_e^{rad} is proportional to $(\bar{n}_e)^3$ and not to $\bar{n}_e$. Second, the multi-machine scaling assumes that radiation comes from a volume that scales as the plasma surface area from experiment to experiment. However, this situation could be different in Tore Supra ED experiments because of the larger divertor volume compared to the main plasma volume. Therefore, in our understanding, the good prediction given by the multi-machine scaling for a large number of tokamaks, including axisymmetric divertor and limiter tokamaks, is consistent with the assumption that in the axisymmetric divertor experiments used for the regression, only a small fraction of the total power is radiated in the divertor volume. The deviation observed on Tore Supra is consistent with the high fraction of divertor radiation, $P_{rad}^{div}/P_{rad}^{div} \approx 80\%$, measured in our experiments.

Therefore, a new scaling has been experimentally derived on Tore Supra from the theoretical basis established in Section 2 for impurity radiation in a region of parallel tranport:

$$P_{rad}^{TS} = \frac{4.5 \times 10^{14}}{\sqrt{Z(Z-1)}} \sqrt{(Z_{eff}-1) f_{sc}} n_e^{div} T_e^{div} \sqrt{\int_{T_e^{div}}^{100} T_e^{0.5} L_Z(T_e)\, dT_e}, \quad (5)$$

where P_{rad}^{TS} is in MW, n_e^{div} in 10^{20} m^{-3}, T_e^{div} in eV, and L_Z in W m^3. This new formulation does not account for the core radiation, but only for the edge and divertor radiation. However such a model is justified in Tore Supra ED plasmas by the experimental finding that divertor radiation is the majority of radiation. In Eq. (5), the impurity concentration in the divertor region, $c_{Z,0}$, which comes in Eq. (4) is replaced by $f_{sc} c_{Z,1}$, where $c_{Z,1}$ is the impurity concentration in the confined plasma, and $f_{sc} = c_{z,0}/c_{Z,1}$ is a screening factor representing the impurity retention in the divertor volume. This screening factor is identical to the divertor exhaust impurity enrichment defined in DIII-D [12] and ASDEX-U [13] in the puff and pump experiments. It is also similar to the penetration factor defined by McCracken [14] for recycling and non-recycling gases. The introduction of f_{sc} in Eq. (5) is necessary when one wants to compare Eq. (4) to experiment, because, experimentally, only the value of $Z_{eff} \approx 1 + Z(Z-1)c_{Z,1}$ in the central plasma region is measured. Assuming that the measured radiated power on Tore Supra is controlled by parallel ion transport (Eqs. (4) and (5)), f_{sc} is calculated by $P_{rad}^{exp} = P_{rad}^{TS}$. The result is plotted versus T_e^{div} in Fig. 7, for the three shots with pure deuterium, nitrogen or neon injection. The radiative power loss coefficient is calculated assuming rapid impurity transport with $n_e \tau_{\|} = 1 \times 10^{16}$ s m^{-3}, and the impurity mixture (C, N, O and Ne) given by spectroscopic measurements. Fig. 7 shows that $f_{sc} \propto \exp[(T_e^{div})^{-\alpha}]$, with $\alpha \approx 1.2$, 1.8 and 2.7 when neon, nitrogen or oxygen is the main radiator respectively. This result also indicates that the screening of oxygen or nitrogen impurities is better than that of neon, since their screening factor decrease more rapidly with increasing electron temperature (in agreement with previous experiments on Tore Supra [15]). This is in agreement with the higher ionization rate coefficient of oxygen and nitrogen.

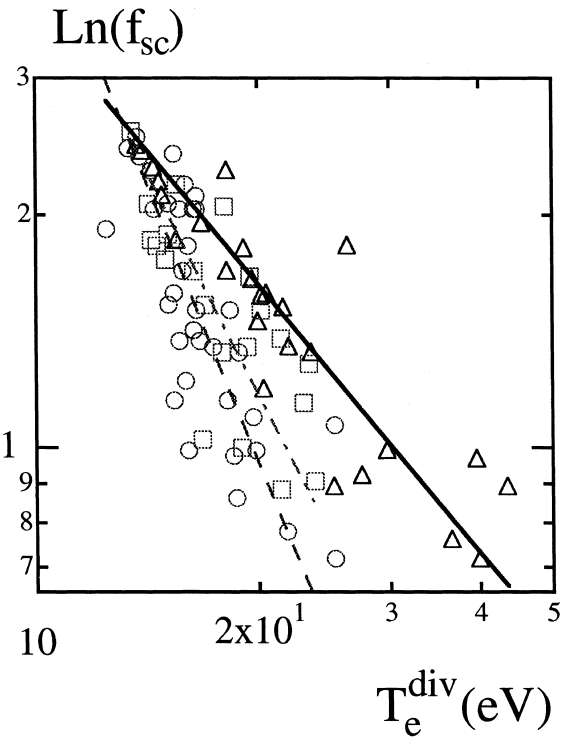

Fig. 7. Screening factor versus target plate temperature, for oxygen (circles, dashed line), nitrogen (squares, dashed-dotted line) and neon (triangles, solid line) radiation.

6. Discussion

The experimental results reported in Sections 4 and 5 are consistent with the following picture.

1. Parallel ion impurity transport plays a minor role in the achieved radiated power. This is supported by the fact that the observed increase of P_{rad} when T_e^{div} decreases from 25 to ≈12 eV (Fig. 5) is much stronger than that predicted by the simple model used throughout this paper (Fig. 1).
2. The analysis of the radiated power scaling through Eq. (5) (Fig. 7) suggests that impurity screening is the dominant mechanism controlling divertor radiation.

7. Conclusion

Highly radiative edge layer experiments in Tore Supra ED plasmas have been reported. The goal was to determine the maximum power that it is possible to radiate in the edge in steady state attached plasma conditions. A comparison is made between high density operation, corresponding to oxygen radiation, and a scenario with nitrogen or neon injection. When oxygen radiation is dominant, a higher radiation fraction is achieved before detachment, $P_{rad}/P_{tot} \approx 88\%$, than in the case where nitrogen is the main radiator, because the maximum of oxygen radiation occurs at a higher electron temperature than that of nitrogen. For the case of neon, detachment is not observed up to $P_{rad}/P_{tot} \approx 83\%$, the target plate temperature remaining higher than ≈15 eV. A 2 s steady state regime has been achieved in these conditions. The radiated power measured in the highly radiating edge regimes obtained in Tore Supra ED plasmas is higher than the prediction of the multi-machine scaling. Such behaviour is consistent with the fact that in the ED configuration of Tore Supra, a large fraction of the radiation originates from the divertor volume where the physics effects are controlled by parallel transport, or with the enhanced impurity screening observed in Tore Supra. Indeed, the new scaling derived for impurity radiation in a region of parallel transport shows that impurity screening on the open field lines is the dominant mechanism controlling divertor radiation.

References

[1] Ph. Ghendrih, Equipe Tore Supra, Plasma Phys. Control. Fusion 39 (1997) B207.
[2] P. Monier-Garbet et al., Proceedings of the 21st EPS Conference, Montpellier, France, Europhys. Conf. Abstr. vol. 18B, 1994, Part II-738.
[3] A. Loarte, Nuclear Fusion 38 (1998) 331.
[4] B. Lipschultz, J. Nucl. Mater. 241–243 (1997) 771.
[5] P.H. Rebut, B.J. Green, Plasma Phys. Contr. Nucl. Fus. Res. 2 (1977) 3.
[6] D. E Post, J. Nucl. Mater. 220-222 (1995) 143.
[7] G. Matthews et al., J. Nucl. Mater. 241–243 (1997) 450.
[8] U. Samm et al., J. Nucl. Mater. 176&177 (1990) 273.
[9] C. Grisolia et al., these Proceedings.
[10] R. Reichle, J.C. Vallet, Proceedings of the 25th EPS Conf., Praha, Europhys. Conf. Abstr., 1998 (to be published).
[11] B. LaBombard et al., J. Nucl. Mater. 241–243 (1997) 149.
[12] M.J. Schaffer et al., J. Nucl. Mater. 241–243 (1997) 585.
[13] A. Kallenbach et al., Nucl. Fusion 35 (1995) 1231.
[14] G.M. McCracken et al., J. Nucl. Mater. 241–243 (1997) 777.
[15] P. Monier-Garbet et al., 14th IAEA Int. Conf. on Plasma Phys. and Controlled Nucl. Fusion Res., Würzburg, 1992, IAEA, Vienna, vol. 1, 1993, pp. 317.